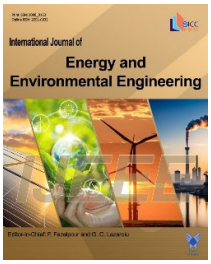

Volume 15, Issue 3, (2024) Article 12

International Journal
of
Energy and Environmental Engineering (IJEEE)

https://doi.org/10.57647/ijeee.2024.1502.09

A Detailed Simulation of a DME/Hydrogen RCCI Engine Performance and Emissions

Mohammad Reza Shafighi[1], Mojtaba Ebrahimi[1,*], Seyed Ali Jazayeri[2]

[1] *Department of Mechanical Engineering, Ayatollah Amoli Branch, Islamic Azad University, Amol, Iran*
[2] *Department of Mechanical Engineering, K. N. Toosi University of Technology, Tehran, Iran*

***Corresponding author:** m.ebrahimi@iau.ir

Original Research

Abstract

The current simulation study seeks to completely eliminate dependence on fossil fuels consumption in a diesel fuel/natural gas RCCI engine. Instead, the engine uses two final products resulting from the natural gas steam reforming process, hydrogen and DME. By changing the engine fuels to non-fossil fuels, the results reveal that along with a 100% reduction in fossil fuel consumption, the total fuel cost per hour of the engine operation will increase by 300%. Compared to diesel fuel/natural gas RCCI engine, the duration of combustion was increased beyond 50 degree crank angle along with the reduction in peak pressure by up to 57 bar. However, a maximum increase of 2.57 bar in indicated mean effective pressure with a gross indicated efficiency of over 55% can be achieved without any concerns about diesel knock. In the hydrogen/DME RCCI engine, carbon dioxide emission can be reduced by up to 157 tons per year in each cylinder. The 2007 EPA and EURO VI levels for formaldehyde and unburned methane are achievable, respectively. Lower than Euro II level for carbon monoxide is unattainable. Moreover, the level of soot and NOx emission lead to the relevant Euro II range due to the chemical properties of DME.

Keywords: RCCI engine; Synthetic fuels; Heavy-duty diesel engine; DME; hydrogen

Cite this article: Shafighi M. R., Ebrahimi M., Jazayeri S. A., A Detailed Simulation of a DME/Hydrogen RCCI Engine Performance and Emissions. Int. J. Energy Environ. Eng. 2024; 15(3): 1-13 https://doi.org/10.57647/ijeee.2024.1502.09

Nomenclature

ATDC	After top dead center
CA	Crank angle
CA_{10}	Crank angle of 10% fuel burned
CA_{50}	Crank angle of 50% fuel burned
CFD	Computational fluid dynamic
CH_2O	Formaldehyde
DME	Di-methyl ether
CO	Carbon monoxide
CO_2	Carbon dioxide
E_{in}	Inlet energy
EGR	Exhaust gas recirculation
EPA	Environmental Protection Agency
EURO	European Emission Standard
EVO	Exhaust valve opening
Exh	Exhaust
GIE	Gross indicated efficiency
H_2	Hydrogen
HCCI	Homogeneous charge compression-ignition
HRR	Heat release rate
IMEP	Indicated mean effective pressure
IVC	Intake valve closing
K	Kelvin
LHV	Lower heating value
m	mass
NOx	Nitrogen oxides
P	Pressure
PPRR	Peak pressure rise rate
PRF	Primary reference fuel
RCCI	Reactivity-controlled compression-ignition
SOC	Start of combustion
SOI	Start of injection
T	Temperature
TDC	Top dead center

UHC	Unburned hydrocarbon
V	Volume
x	Mass fraction

1. Introduction

The greater demand for carbon-based fuels energy causes increasing environmental challenges. One of the challenges ahead is global warming from the production of more carbon dioxide. A suitable solution to reduce carbon dioxide production is to reduce the use of hydrocarbon fuels with high-carbon content in various sectors and replace them with low-carbon content fuels or carbon-free fuels. Among the various sectors, the transportation sector (air, marine, railway, and road) is an important part of energy consumption, especially from conventional fossil fuels. Heavy-duty diesel engines are widely used in this important sector. Unfortunately, related to environmental issues, the use of diesel engines has adverse effects on humans and the environment. Because these engines use conventional diesel combustion strategy and consume high-carbon content fuels, they produce well-known emissions [1]. The problem of these engines' emissions can be limited by using after-treatment equipment. But, one of their drawbacks is the increase in costs and fuel consumption in the engine. Therefore, replacing higher-carbon bond fuel types with lower-carbon fuel types was considered, as a solution. This was the beginning of the dual-fuel engines.

A dual-fuel engine can operate with conventional diesel fuel alone or simultaneously with it and a gaseous type fuel as a main fuel. In these engines, gaseous fuel is mixed with the intake air through the air inlet port injection. The direct diesel fuel injection inside the engine cylinder supplies the ignition energy for the presence air-gaseous fuel mixture [2]. Natural gas, which is a low-carbon content gaseous fuel, is available worldwide and is considered a sustainable energy solution until 2050. Given the advantage of low-risk storage of natural gas, this fuel is a good candidate for use in these engines. The performance of dual-fuel engines is comparable with that of diesel engines, and even better than them in the medium to full-load range. The emission level of natural gas fueled engines under dual-fuel combustion is lower than diesel engines. However, they are prone to releasing unburned hydrocarbons and carbon monoxide in high levels. Also, these engines' efficiency is lower in the low-load range. Therefore, it is preferable dual-fuel mode of combustion shifts to diesel mode in low-load [2].

Another problem with dual-fuel engines that use diesel fuel and natural gas is unburned methane as a contributing factor to global warming [3]. Moreover, any disruption in the complete oxidation of natural gas (i.e., unburned methane formation) will lead to the formation of toxic and carcinogenic gases such as formaldehyde [3]. Given the diesel fuel consumption as an ignition promoter in mentioned engines (conventional and dual-fuel), NOx and soot formation during the combustion process is not unexpected. One of the factors influencing the formation of nitrogen oxides is temperature greater than 1900 K inside the engine cylinder. Moreover, fuel-rich areas resulting from the diesel fuel injection causes that these engines are susceptible to the production of soot at a high level. Efforts to identify the factors producing the aforementioned emissions led to the emergence of the premixed low-temperature combustion strategy [4].

A subset of the premixed low-temperature premixed combustion strategy, namely RCCI combustion, operates similarly to dual-fuel engines. RCCI engines also use the idea of premixing the intake air with a low-reactivity fuel, firstly and then injecting a high-reactivity fuel inside the combustion chamber [5]. The main combustion initiation in dual-fuel engines completely depends on thermodynamic conditions. In contrast, the start of main combustion in RCCI engines depends on chemical reactions between several chemical species. Research results related to RCCI combustion have shown that, in addition to increasing thermal efficiency, the levels of soot and nitrogen oxide emissions have also decreased significantly [5].

Although using various combustion strategies in heavy-duty diesel engines has significantly reduced emissions levels and improved the combustion process [6-11], the problem of global warming caused by the fossil fuels consumption still exists. Because, the result of using common hydrocarbon fuels at an economical price by these engines is the release of greenhouse gases into the environment. Therefore, reducing the consumption of high-carbon content fuels, like diesel fuel, or low-carbon content fuels, like natural gas, and replacing them with renewable fuels with carbon-free fuels, such as hydrogen, is an inevitable necessity.

Compared to conventional fossil fuels, hydrogen requires very little energy to ignite [12]. Hydrogen is highly permeable and is desirable for the purposes of forming homogeneous mixtures. This property minimizes the occurrence of unsafe conditions when hydrogen leaks in a system. Due to the characteristic of hydrogen in relation to high auto-ignition resistance (585 °C), higher compression ratios are achievable in engines. The distance of the wall quenching effect on the hydrogen flame is much shorter than that of other common fossil fuels [12]. Therefore, the flame created by hydrogen is able to approach to an engine's cylinder wall before the hydrogen flame is extinguished by the effect of this phenomenon. Therefore, the combustion efficiency by hydrogen consumption is expected to be much higher. Hydrogen flame velocity is faster than that of commercial hydrocarbon fuels. Thus, it is expected that releasing the available fuel energy will be faster during the combustion process and the duration of combustion will be much lower.

Hydrogen is not freely available in nature, and various methods are used to produce it. Due to the increasing demand for hydrogen in various industries, the current large-scale production of hydrogen is highly dependent on fossil fuels (approximately 96%). Among fossil fuels,the cheapest method of producing hydrogen is through the reforming process of natural gas.

Natural gas reforming process is divided into three different methods, including dry reforming, steam reforming, and partial oxidation. Among the three aforementioned reforming methods, the natural gas reforming method through steam (Figure 1) accounts for 75% of hydrogen production in the world, and this type of hydrogen produced is called gray hydrogen [13]. One of the disadvantages of this method is that it produces 13.3 times the weight of hydrogen as carbon dioxide (i.e., global warming concern), and the process efficiency is less than 60%.

As can be seen in Figure 1, another important point in natural gas reforming processes is that the final product is not pure hydrogen but is hydrogen along with carbon monoxide in different volumetric ratios (i.e., syngas). In the dry natural gas reforming method, the ratio of H_2 to CO is one; in the natural gas reforming method by steam, it is three, and in the partial oxidation method, this ratio is two. If the goal is to produce hydrogen with a higher volume percentage than carbon monoxide, along with the aforementioned reforming methods, chemical reactions between water and carbon monoxide is necessary to regenerate hydrogen (i.e., water-gas shift reaction). Using this method, the ratio of H_2 to CO can be enhanced to more than six. However, carbon dioxide will also be produced along with the oxidation of carbon monoxide. Considering the significant challenge of natural gas fueled dual-fuel and RCCI engines, enriching natural gas with hydrogen or syngas can be a proper method to overcome the engine emissions, especially greenhouse gas emissions like carbon dioxide and unburned methane [14-18].

Although, syngas produced from the natural gas reforming process can be used as a fuel, it can be also utilized through processes like synthesis and distillation to produce synthetic chemical species such as di-methyl ether (DME) and methanol [19] (Figure 1). Methanol is used in many applications, like the production of polymers, hydrocarbon fuels like gasoline, and solvents. Methanol has octane number higher than that of gasoline, thus, it can be consumed as a low-reactive fuel in an RCCI engine [20]. On the other hand, DME, which is widely used in the chemical industry and sprays, with the properties presented in Table 1, is capable of being a suitable alternative to high-reactive fuels (like diesel fuel) [21-31]. There are no carbon-carbon bonds in di-methyl ether's molecular structure, and DME contains about 35% oxygen. This synthetic fuel is not considered a global warming problem.

Recently, limited studies have also been conducted in relation to using hydrogen as a sole fuel instead of hydrocarbon gaseous fuels in RCCI engines [32-35]. The results indicate that using hydrogen instead of natural gas can enhance combustion efficiency and decrease challenging emissions in RCCI engines. However, due to the necessity of high-reactive diesel fuel consumption in hydrogen-fueled engines, these engines are still dependent on hydrocarbon fuel consumption and are prone to forming well-known emissions, mainly CO_2, soot, and UHC.

Therefore, following the previous works of the present authors in using pure hydrogen as a sole low-reactive fuel in an RCCI engine [32]; the current simulation study seeks to directly and completely eliminate dependence on fossil fuels consumption in an RCCI engine. Therefore, as shown in Figure 2, two final products from the natural gas steam reforming process, namely hydrogen and DME, are used as low-reactive and high-reactive fuels in the RCCI engine. Carbon dioxide, a known greenhouse gas formed in natural gas reforming process, will be also used as effective diluents (i.e., simulated EGR) in controlling the engine in-cylinder temperature. The main objective of this study is to control the combustion process and reduce the potential for well-known engine emissions formation as much as possible through the use of non-fossil fuels.

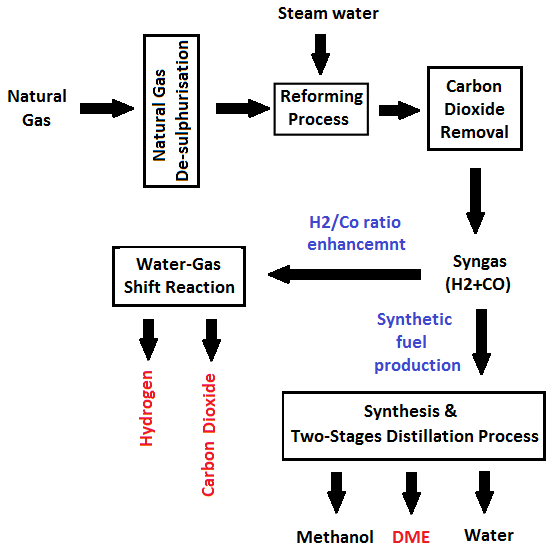

Figure 1. Natural gas reforming process by steam water

Table 1. DME properties compared to diesel fuel [22]

Fuel type	Diesel fuel	DME
Molar mass (g/mole)	170.0	46.0
Carbon mass in fuel structure (%)	86.8	52.2
Hydrogen mass in fuel structure (%)	14.0	13.0
Oxygen mass in fuel structure (%)	0	35.0
Ratio of carbon to hydrogen	0.52	0.34
Density in liquid state (Kg/m^3)	831.0	667.0
Fuel cetane number range	40-50	Over 55
Auto-ignition T (K)	523	508
Specific heat capacity (KJ/kg K)	1.7	3.0
Air/fuel ratio (% mass)	14.6	9.0
LHV of fuel (MJ/kg)	42.0	27.6
Atmospheric boiling temperature (K)	Max. 643	248

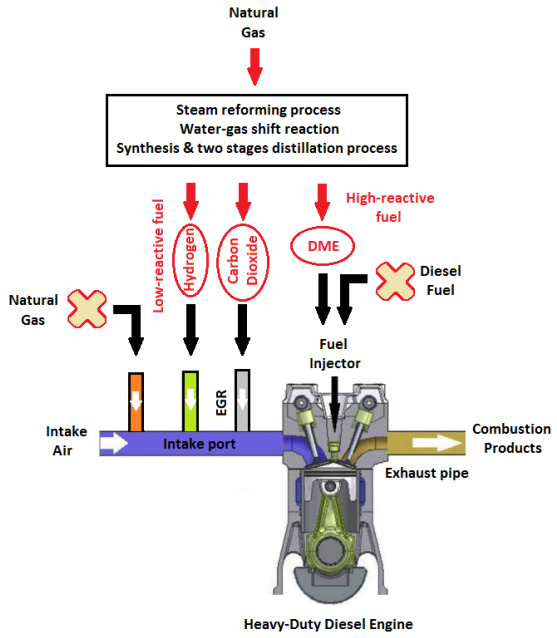

Figure 2. The idea of completely elimination of fossil fuels consumption in a heavy-duty diesel engine

Table 2. Some important parameters in the selected RCCI engine [9]

Type of engine	Single-cylinder
Piston bowl geometry	Bathtub
Combustion mode	RCCI combustion
Hydrocarbon fuels type	Natural gas Diesel fuel ($CH_{1.76}$)
Cylinder bore /Stroke (mm)	137.2/165.1
Compression ratio	14.88:1
Speed (rpm)/Swirl ratio	1300 (constant)/0.7
Connecting rod length (mm)	261.6
Valves No. (Intake and Exhaust)	2
Valves timing (° ATDC)	IVC: - 143 EVO: +130
NG injection mechanism	Intake air port fuel injection
Injector parameters (Common rail mechanism, 500 bar fuel spray pressure)	6 (holes No.) 250 µm (holes diameter)

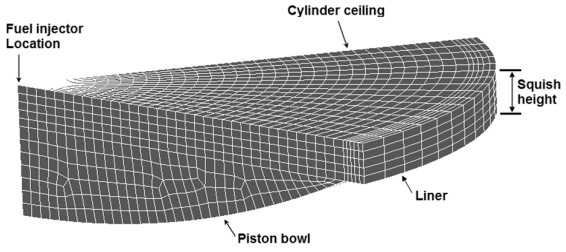

Figure 3. Created combustion chamber's computational model

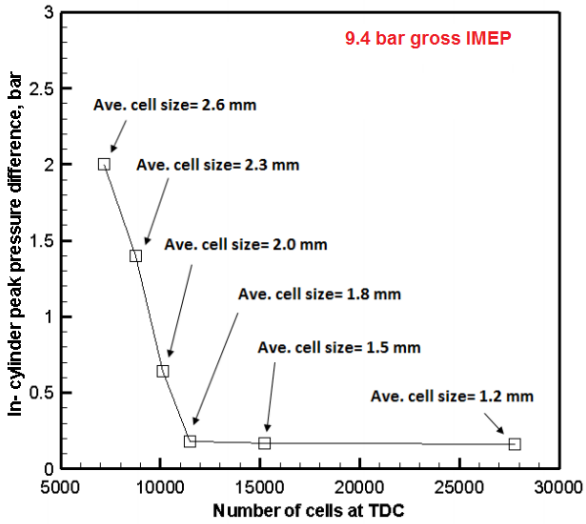

Figure 4. Computational grid independency analysis

Table 3. Details of the used CFD solver setting

Characteristic	Setting ranges
Time step (Crank angle step for constant engine speed)	From the intake valve closing to before high-reactive fuel injection: 2 degree crank angle After fuel injection until combustion initiation: 1 degree crank angle After combustion occurrence up to 30 degrees after it: 0.5 degree crank angle 30 degree after the combustion initiation up to the exhaust valve opening: 1 degree
Turbulence dispersion model	O'Rourke model: Turbulence kinetic energy: 1 m^2/S^2 Turbulence length scale: 0.00137 m Turbulence dissipation rate: 120 m^2/S^3
Convergence tolerance criteria per crank angle	Max. number of iterations: 60 Min. number of iteration: 5 Pressure tolerance: 0.01 Momentum tolerance: 0.01 Turbulence kinetic energy: 0.01 Turbulence dissipation rate: 0.01

2. Single-Cylinder RCCI Engine Specifications

The specifications of natural gas/diesel fuel RCCI engine under investigation are listed in Table 2 [9]. To conduct a closed-cycle combustion simulation, the computational model shown in Figure 3 was created through the AVL FIRE CFD tool. Moreover, for a selected engine load, i.e., 9.4 bar gross IMEP, the mesh

independency criteria of the created computational model of the natural gas/diesel fuel RCCI engine's cylinder was checked and presented in Figure 4. For this purpose, several different sizes were chosen for the computational model cells. For the selected engine load, the obtained peak pressure from the combustion simulation was compared with that of the experimental data [9]. As depicted in this figure, in terms of combustion simulation accuracy and computational time, an average cell size of 1.8 mm is considered to be the optimal size.

In Table 3, some of the used CFD solver setting were presented.

Also, to predict all chemical reactions between two used hydrocarbon fuels in the selected engine (i.e., natural gas and diesel fuel), it is necessary to couple another chemistry tool with the implemented CFD tool like CHEMKIN tool. In order to implement CHEMKIN tool, a reduced PRF mechanism including 76 species and 464 reactions was also chosen [36]. It should be noted that in this selected reduced PRF mechanism, chemical reactions between n-heptane and methane are considered instead of diesel fuel and natural gas, respectively. Also, to better evaluation the diesel fuel spray behavior, some essential sub-models were considered as listed in Table 4.

According to the test conditions listed in Table 5, this selected engine was examined by Walker et al. [9], without any use of exhaust gas recirculation and assuming a constant equivalence ratio of 0.3.

The only reliable information reported from the mentioned engine testing for use in validating combustion simulation results is: the value of maximum pressure, the PPRR, the diagram of HRR, and the CA50 location. Figure 5 shows a comparison between RCCI combustion simulation results (including maximum pressure and PPRR) and the experimental data [9]. In terms of peak pressure, comparing the simulation results reveals the accuracy of the created computational model for understanding RCCI engine behavior. Moreover, the obtained simulation results related to the PPRR indicate that the difference in results is less than 3.5 bar without any risk of diesel knock (i.e., below 15bar/° CA [42]).

Comparing the HRR obtained from the current simulation and test results is shown in Fig. 6. One of the well-known phenomena that are expected after direct injection of normal-chain fuels (like diesel fuel) into an engine combustion chamber is the occurrence of a cool flame (i.e., low-temperature oxidation). The cool flame or the location of releasing 10% of the fuel energy (i.e., CA10) can be seen in Figure 6. Research has confirmed that a cool flame occurs when the temperature inside the engine cylinder is around 750 K to 800 K, about 10 to 20º crank angle before the main combustion initiation [43]. In the current simulation study, n-heptane with a lower initial boiling point than commercial diesel fuel is used. Hence, as depicted in Fig. 6, this phenomenon happens slightly earlier compared to the engine test conditions, but, between 10 to 20º CA before the start of main combustion.

Another important factor in evaluating the HRR is the start of main combustion (i.e., high-temperature oxidation). The first stage of energy release is initiated by high-reactive fuel (i.e., n-heptane). In comparison to commercial diesel fuel (i.e., $CH_{1.76}$), normal heptane has a higher cetane number; hence, the rate of n-heptane energy releasing will be steeper. After this stage, the stage of methane energy releasing is initiated, as low-reactive fuel. Considering the small deviation between the HRR diagrams, it is very effective to evaluate the location of CA50. Under RCCI engine test conditions [9], the CA50 location was set to be at the TDC position (i.e., 0º ATDC). As depicted in Figure 7, due to the n-heptane properties compared to commercial diesel fuel in terms of its earlier heat release rate and lower boiling point, the CA50 position occurs before the TDC.

Table 4. Details of selected sub-models

Behavior type	Selected model
The effect of turbulent eddies on the diesel fuel droplet	Gosman [37]
Diesel fuel spray and engine cylinder wall interaction	Wall jet [38]
Evaporation of diesel fuel droplets	Dukowicz [39]
Break-up of diesel fuel droplets	Wave standard [40]
Diesel fuel flow through out nozzle	Reitz [41]

Table 5. Engine operating conditions on the test-bench [9]

Inlet P (bar)/	0.97/	1.08/	1.32/	1.60/	1.90/	2.20/
Inlet T (K)/	313/	313/	313/	313/	313/	313/
Gross IMEP (bar)	5.6	6.3	7.7	9.4	11.5	13.5
Fuels mass:						
Diesel (mg)/	13/	13/	13/	13/	13/	13/
NG (mg)/	42/	49/	62/	76/	96/	108/
Total (mg)/	55/	62/	75/	89/	109/	121/
Equivalence ratio	0.3	0.3	0.3	0.3	0.3	0.3
Fuel injection:						
NG/	Port/	Port/	Port/	Port/	Port/	Port/
diesel (º ATDC)	-35	-39	-42	-45	-48	-51

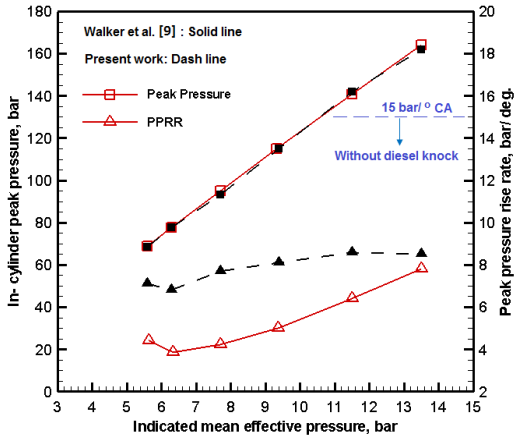

Figure 5. Comparison of RCCI combustion simulation and experimental results related to maximum pressure and PPRR

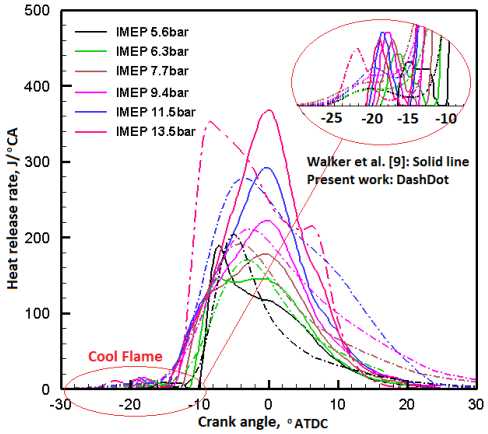

Figure 6. Validation of simulation results in terms of the HRR

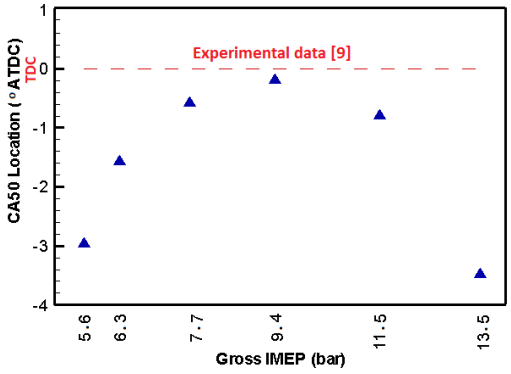

Figure 7. CA50 location assessment

However, compared to the experimental results [9], the maximum deviation for the CA50 location is only about three degrees crank angle. Considering the aforementioned parameters, the created computational model has a proper accuracy, thus, the simulation process will continue with this computational model.

3. Adjusting DME/Hydrogen RCCI Engine Operating Conditions

In the present study, based on the constant overall fuel energy contents, the engine operating conditions to completely eliminate the consumption of fossil fuels are presented in Table 6. As listed in this table, the diesel fuel/NG RCCI engine test setting is considered as case No. 1 [9]. To better evaluate the fossil fuel-free engine performance, as depicted in Fig. 8, hydrogen is initially completely replacing natural gas with equivalent energy content (case No. 2) in the first step. Of course, in these cases, the mass of diesel fuel is assumed to be the same and the difference in the total fuel energy content was corrected by the mass of hydrogen. Then, in the second step, diesel fuel as the energy supplier for the ignition of the air-hydrogen mixture will be replaced by DME of the same mass. Due to the lower LHV of DME compared to commercial diesel fuel, the difference in total fuel energy content was compensated by hydrogen (case No. 3). Compared to diesel fuel properties (Table 1), DME has a higher cetane number; hence, to obtain a maximum engine load, the DME injection timing must be shifted towards the TDC position [21]. Also, in order to DME injection in liquid phase, its injection temperature must be less than its boiling point.

To conduct combustion simulation in case No. 2, due to the rapid release of hydrogen energy, the use of diluents of the air-hydrogen mixture (i.e., the EGR and nitrogen addition) is a necessity [32]. Therefore, to improve the considered reduced PRF mechanism [36], using other chemical mechanisms to predict all reactions between hydrogen, nitrogen, carbon dioxide, and carbon monoxide is needed [44-46] (Table 7). Moreover, when replacing diesel fuel with DME, it is also necessary to use a reduced PRF mechanism covering all reactions between DME and hydrogen [49] (Table 7).

4. Results and Discussion

4.1. Economic Assessment of Fuel Costs

By completely replacing hydrocarbon fuels, a 100% reduction in the fossil fuel consumption can be achieved (Figure 9). However, given the price of 1.18 USD/kg of diesel fuel, 0.84 USD/kg of DME, 1.95 USD/kg of hydrogen [48], and 0.223 USD/kg of natural gas (on average), the total fuel cost per hour of engine operation fueled with hydrogen and DME will increase by 300%. It should be noted that, given the trend of developing hydrogen production in the world, the price of this green fuel will decrease significantly in the coming years. Therefore, the cost of replacing synthetic fuels in engines will become more economical [48].

4.2. The Hydrogen/DME RCCI Engine Combustion Characteristics Assessment

As mentioned earlier, the demonstration of the cool flame phenomenon is one of the important characteristics of the direct injection of normal chain hydrocarbon fuels. In case No. 2, earlier injection of diesel fuel is considered as a combustion phasing control strategy. Therefore, due to the greater effect of air swirl on reduction of high-reactivity fuel-rich areas, the amount of fuel energy released is reduced drastically when a cool flame occurs. By replacing diesel fuel with

DME, this phenomenon does not occur because DME is not a normal-chain hydrocarbon fuel (Figure 10). On the contrary, since DME is more auto-igniting than diesel fuel, the DME vaporization and combustion initiation occur simultaneously, without any noticeable delay compared to commercial diesel fuel.

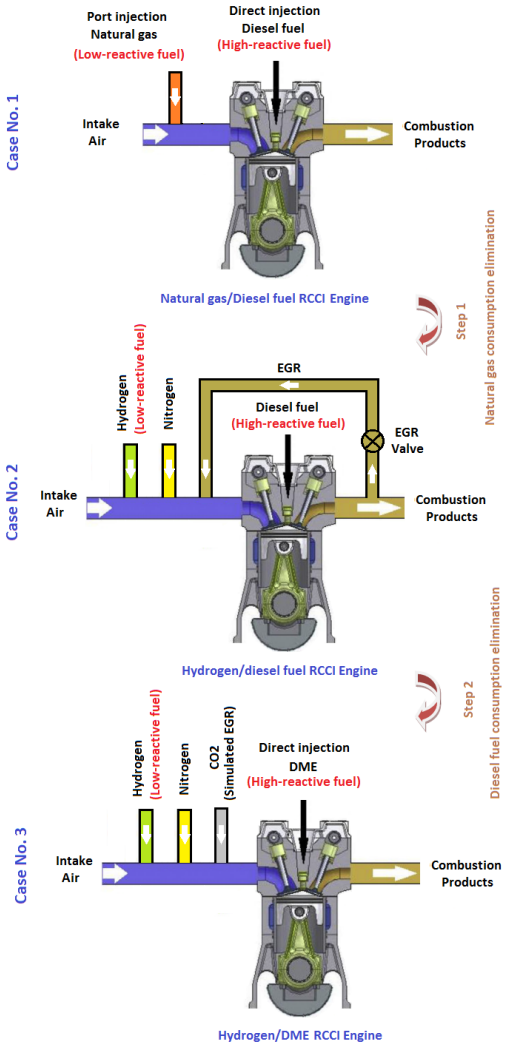

Figure 8. Phasing out fossil fuels in the engine under evaluation

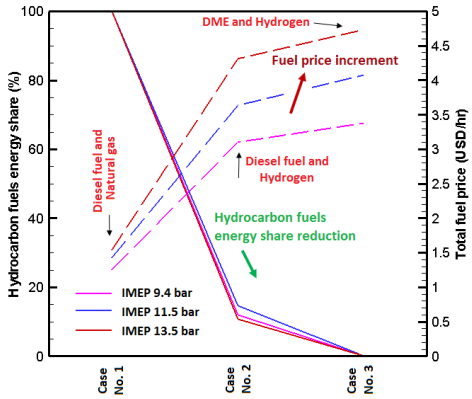

Figure 9. Economic assessment of eliminating the use of hydrocarbon fuels at the engine's mid-load range

Table 6. Engine operating conditions for conducting the present simulation

Case No. 1: Natural gas/Diesel RCCI Engine [9]				
Gross IMEP (bar)		9.4	11.5	13.5
Fuel mass	Diesel fuel (mg)	13	13	13
	Natural gas (mg)	76	96	108
Total fuel energy content (J)		4380	5380	5980
EGR (%)		0	0	0
Diesel fuel SOI (° ATDC)		-45	-48	-51
Diesel fuel injection temperature (K)		330	330	330
Case No. 2: Hydrogen/Diesel RCCI Engine				
Fuel mass	Diesel fuel (mg)	13	13	13
	Hydrogen (mg)	31.7	40.05	45.04
Total fuel energy content (J)		4380	5381	5979
N2 addition/H_2 volume ratio (%)		50	50	50
EGR (%)		6	7	8
Diesel fuel SOI (° ATDC)		-68	-70	-71
Diesel fuel injection temperature (K)		330	330	330
Case No. 3: Hydrogen/DME RCCI Engine				
Fuel mass	DME (mg)	13	13	13
	Hydrogen (mg)	33.53	41.88	46.89
Total fuel energy content (J)		4379	5380	5980
N2 addition/H_2 volume ratio (%)		50	50	50
EGR (%)		6	7	8
DME SOI (° ATDC)		0	0	0
DME injection temperature (K)		220	220	220

Table 7. Details of selected reduced PRF mechanisms and engine emissions modules

Engine fuels type	Selected PRF mechanism
Natural gas and diesel fuel without any EGR	Rahimi et al. [36] with 76 species and 464 reactions
Hydrogen and diesel fuel with EGR and nitrogen addition	Rahimi et al. [36] with considering San Diego [44] and Li et al. [45] mechanisms with 53 reactions for nitrogen and Davis et al. mechanism [46] with 30 reactions for carbon dioxide (i.e., EGR)
Hydrogen and DME with EGR and nitrogen addition	Platz et al. mechanism [47] with 79 species and 351 reactions with considering Davis et al. mechanism [46] with 30 reactions for carbon dioxide. NOx emission model: Zeldovich model Soot emission model: Kennedy/ Hiroyasu/ Magnussen model

The location of CA50 was also evaluated, as one of the important combustion characteristics. As shown in Fig. 10, when using diesel and natural gas in the aforementioned engine [9] (case No. 1), the CA50 occurs at the top dead center. In case No. 2, when the required energy for air-hydrogen mixture combustion initiation is provided by diesel fuel, the dilution of the intake mixture (contains air and hydrogen) along with advancing the time of diesel fuel injection are necessary to control the air-hydrogen mixture combustion. Therefore, a delay in the main combustion initiation occurs and the combustion process and, as a result, the CA50 location will be shifted to the expansion stroke (Figure 10).

On the other hand, when diesel is completely replaced with DME (case No. 3), due to the properties of DME mentioned earlier, it is injected at the TDC position to control combustion phasing. Therefore, as listed in Table 8, the location of CA50 will be shifted to more than 15 degrees of crank angle after the TDC. As a result, the expansion work effect and reduction in the rate of chemical reactions (i.e., combustion rate), the combustion duration has increased by about two times compared to the experimental results [9] (i.e., more than 50 degrees of crank angle). On the contrary, according to the results presented in Figure 10, the expansion work affects the combustion characteristic, hence; a reduction in peak in-cylinder pressure occurs by up to 30%. However, the fossil fuel-free engine's IMEP can be increased by up to 27%. Meanwhile, the PPRR in the combustion process will be below its permissible range (i.e., 15bar/° CA [42]), without any diesel knock.

4.3. Fuel Energy Balance Analysis

The energy balance in the combustion process has also been analyzed. For this purpose, important parameters such as gross indicated efficiency, energy loss due to inefficient combustion processes, energy loss due to the exit of high temperature combustion products, and energy loss due to heat transfer through the use of coolant, lubricant, and environment have been considered. The gross indicated efficiency for each case was calculated through Equation 1 [14].

$$\eta_{GIE} = \frac{Grosswork}{E_{in}} = \frac{\int_{-180^\circ}^{+180^\circ} PdV}{E_{in}} \quad (1)$$

$$E_{in} = m_{fuel}\left[(x \cdot LHV)_{hydrogen} + (x \cdot LHV)_{\substack{dieselfuel \\ orDME}}\right]$$

The presence of carbon monoxide and unburned hydrocarbons at the end of the combustion process is considered as energy loss due to combustion inefficiency. This type of energy loss can be derived through Equation 2 [14].

$$\eta_{Combustionloss} = \frac{(\dot{m} \times LHV)_{CO} + (\dot{m} \times LHV)_{UHC}}{(\dot{m} \times LHV)_{fuel}} \quad (2)$$

Also, high temperature combustion products discharge to the exhaust port indicates another type of energy loss (Equation 3). The main content of combustion products is considered to be oxygen, CO, UHC, nitrogen, CO_2, water vapor, and NOx [14].

$$\eta_{Exhaustloss} = \frac{\dot{m}.[Enthalpy(T_{exhaust}) - Enthalpy(T_{intake})]}{(\dot{m} \times LHV)_{fuel}} \quad (3)$$

Since in the closed combustion cycle simulation process (i.e., from the IVC to the EVO), energy losses due to the use of lubricating oil and coolant, and heat exchange with the environment cannot be measured, Equation 4 is used to calculate this type of energy losses [5,14].

$$\eta_{\substack{Heattransfer \\ loss}} = 100 - \left(\eta_{GIE} + \eta_{\substack{Exhaust \\ loss}} + \eta_{\substack{Combustion \\ loss}}\right) \quad (4)$$

According to the HRR presented in Figure 10, compared to the case of using fossil fuels (case No. 1), in the other two cases, intake air-fuel mixture dilution delays the main combustion initiation. As listed in Table 8, in the case No. 2, along with reducing in the combustion duration, a delay in the combustion initiation also occurs. Based on the P-V diagrams depicted in Figure 11, due to the faster heat release of hydrogen energy, the achieved work in the same fuel energy content is lower for case No. 2; hence, the gross indicated efficiency is reduced (Table 8). However, the temperature of combustion products increases significantly at the EVO. Thus, it is expected that the amount of energy losses due to the discharge of combustion products will also increase. In contrast, the combustion rate increases due to the increase in the in-cylinder temperature in the entire engine cylinder (Figure 11). In other words, energy losses due to combustion inefficiency will be significantly reduced.

When using DME instead of diesel fuel along with the use of hydrogen, the overall combustion process is extended further into the engine's expansion stroke. In this case, the in-cylinder peak temperature drops sharply. Hence, the engine's combustion duration increases by up to two times due to the reduction in the oxidation rate. As shown in Figure 10, due to the slower heat release of fuel energy, the achieved work in the same fuel energy content is higher for case No. 3; hence, based on Equation 1, the gross indicated efficiency is increased (Table 9). Although the gross indicated efficiency increases to over 55%, the temperature of the combustion products will be above 1000 K when the exhaust valve opens. Therefore, the energy losses due to the release of combustion products will be higher.

In contrast, as can be seen in Figure 12, when using DME as a high-reactive fuel, the temperature close to the engine cylinder wall reduces sharply. Therefore, energy losses due to the increased potential for the formation of carbon monoxide and unburned hydrocarbon in these areas will increase. A comparative diagram of the energy balance when fossil fuels are completely replaced by synthetic fuels is presented in Figure 13.

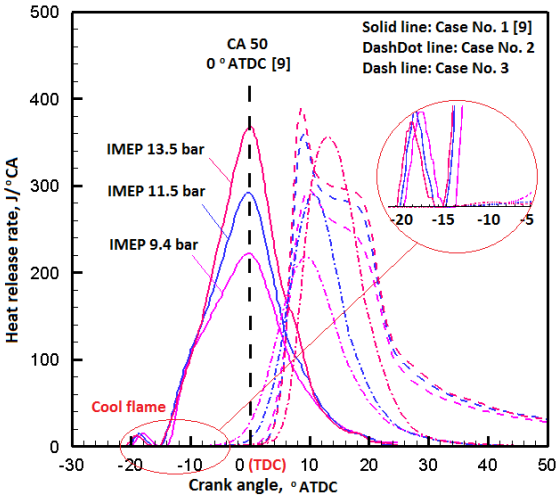

Figure 10. The HRR comparison by replacing hydrocarbon fuels with synthetic fuels

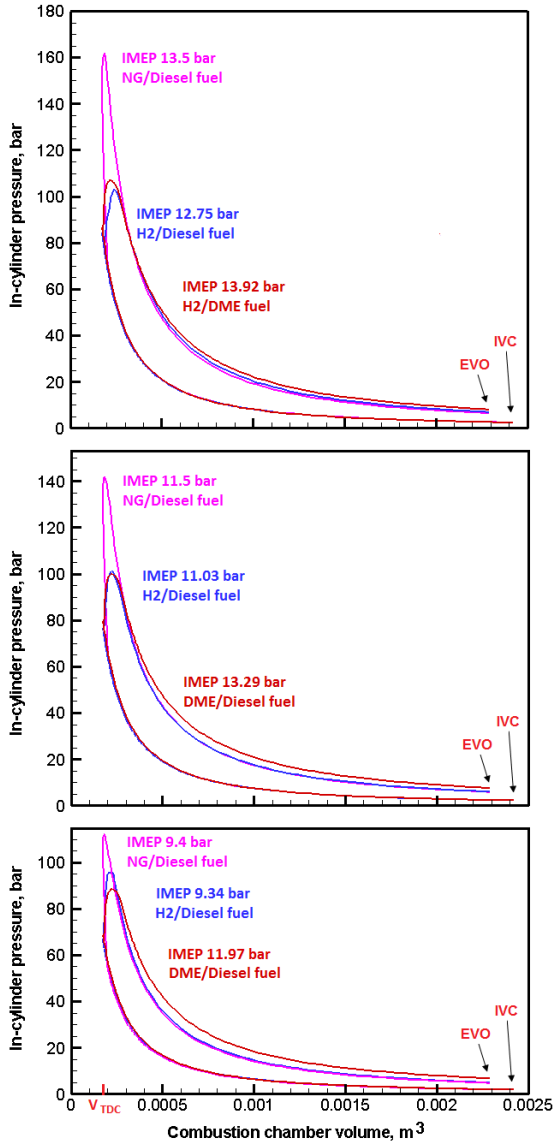

Figure 11. P-V diagrams comparison for three cases

Table 8. Engine combustion characteristics evaluation

Case No. 1: Natural gas/Diesel RCCI Engine [9]			
IMEPs at mid-load (bar)	9.4	11.5	13.5
CA50 (° ATDC)	0	0	0
Combustion duration (° CA)	25	25	25
In-cylinder peak pressure (bar)	115	141	164
PPRR (bar/° CA)	5.0	6.4	7.8
Case No. 2: Hydrogen/Diesel RCCI Engine			
Obtained IMEPs at mid-load (bar)	9.34	11.03	12.75
CA50 (° ATDC)	8.5	11.5	14.5
Combustion duration (° CA)	14.0	16.5	19.5
In-cylinder peak pressure (bar)	96	101	103
PPRR (bar/° CA)	4.8	4.6	3.9
Case No. 3: Hydrogen/DME RCCI Engine			
Obtained IMEPs at mid-load (bar)	11.97	13.29	13.92
CA50 (° ATDC)	15.5	16.5	17.0
Combustion duration (° CA)	57	56	55
In-cylinder peak pressure (bar)	88.4	100	107
PPRR (bar/° CA)	5.9	5.7	6.3

Table 9. Calculated gross indicated efficiency for each case

Case No. 1: Natural gas/Diesel RCCI Engine [9]			
IMEPs (bar)	9.4	11.5	13.5
In-cylinder peak temperature (K)	1787	1863	1905
Exhaust temperature (K)	913	915	923
GIE (%)	52.3	52.1	55.1
Case No. 2: Hydrogen/Diesel RCCI Engine			
IMEPs (bar)	9.34	11.03	12.75
In-cylinder peak temperature (K)	1890	1875	1870
Exhaust temperature (K)	974	1016	1086
GIE (%)	50.8	49.7	48.4
Case No. 3: Hydrogen/DME RCCI Engine			
IMEPs (bar)	11.97	13.29	13.92
In-cylinder peak temperature (K)	1569	1533	1501
Exhaust temperature (K)	1136	1100	1069
GIE (%)	60.7	58.3	56.8

Table 10. DME oxidation pathway

Obtained IMEPs (bar)	11.97	13.29	13.92
Max. temperature (K)	1569	1533	1501
NOx (g/kWh)	7.9	6.3	5.6
CO (g/kWh)	4.42	3.89	3.97
Unburned Methane (g/kWh)	2E-10	8E-11	8E-11
Soot (g/kWh)	0.12	0.06	0.05
Formaldehyde (g/kWh)	7E-7	1E-6	6E-7
CO2 reduction (g/each cycle) (Tons/year)	0.17 (58.1)	0.37 (126.4)	0.46 (157.2)

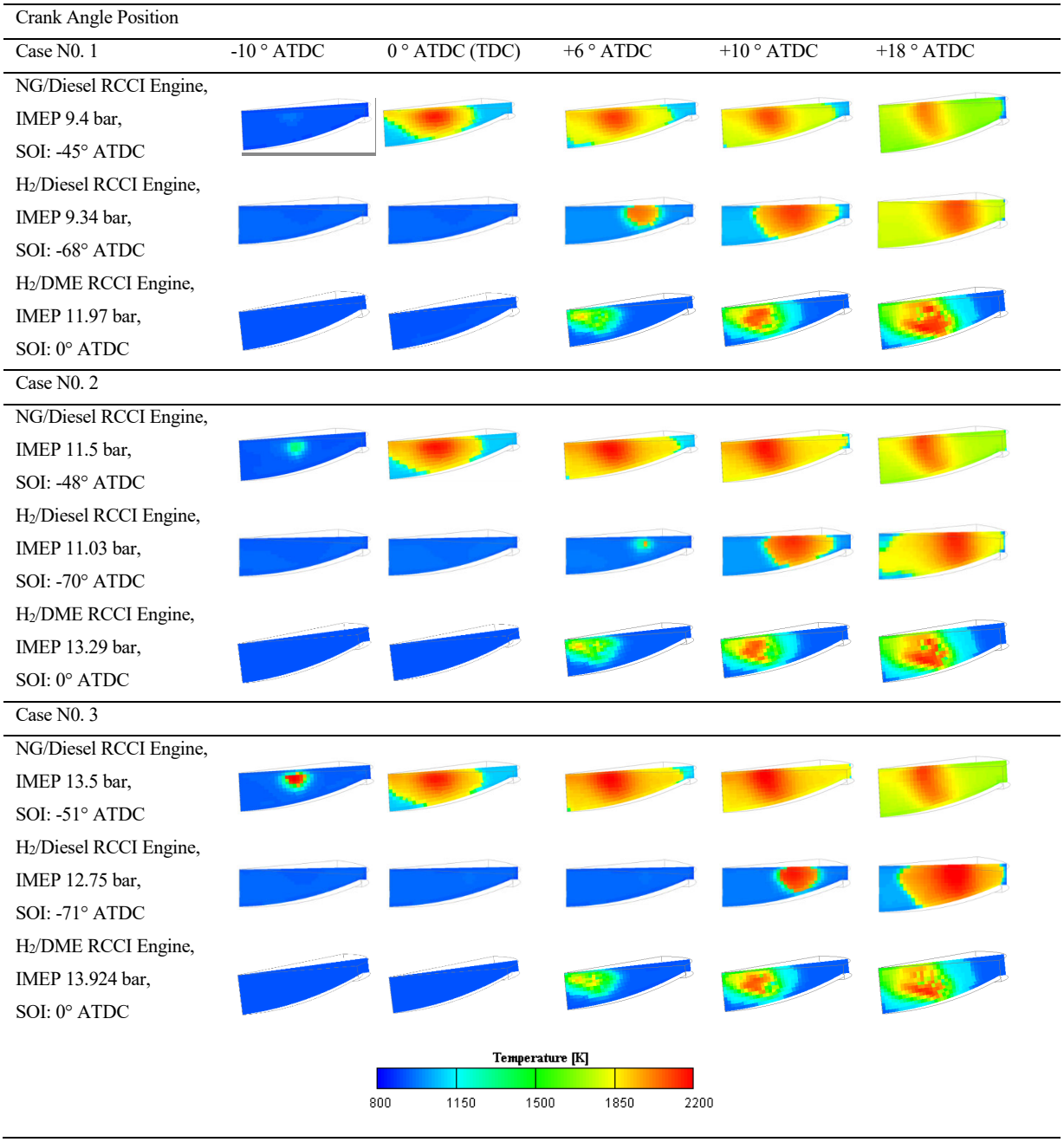

Figure 12. Temperature contour for three cases

4.4. The Fossil Fuel-Free Engine Emissions Assessment

To analyze the effect of replacing conventional fossil fuels with synthetic fuels on the engine emissions, the oxidation pathway of synthetic fuels was evaluated.After DME injection into the engine combustion chamber containing an air-hydrogen mixture, the hydrogen is decomposed and consumed according to the following reactions.

$$O + H_2 \longrightarrow OH + H \quad (5)$$

$$H_2 + OH \longrightarrow H_2O + H \quad (6)$$

As shown in Figure 14, with the presence of important radicals such as H, OH, and O, di-methyl ether loses hydrogen in its molecular bond to form the methoxy methyl radical (CH_3OCH_2). The methoxy methyl radical decomposition causes forming two vital species, namely formaldehyde (CH_2O) and methyl radical (CH_3) that continue the DME decomposition pathway.

In natural gas-fueled engines, the cause of formaldehyde formation is due to the insufficient natural gas combustion, directly [3]. However, in a DME/Hydrogen engine, due to natural gas replacement with hydrogen, the only source of formaldehyde production is through the DME oxidation. On the other hand, in this process, the methyl radical is directly

related to the formation of methane. It is predicted that all the methane formed in the oxidation of DME will be converted back to the methyl radical. However, if this reverse reaction does not occur completely and the formed methane is not consumed in the combustion process, the formation of unburned methane as an important emission is not far from expected.

According to the DME oxidation pathway depicted in Figure 14, by eliminating the fossil fuels consumption, CO_2 is formed only through DME oxidation. Thus, assuming continuous engine operation for 24 hours (such as power generation purpose), the amount of CO_2 emitted can be reduced by up to 157 tons/year for a single-cylinder engine, compared to case No. 1 [9].

The hydrogen/DME RCCI engine emission levels are presented in Table 10. As can be seen, the emission levels of unburned methane resulting from the DME oxidation process are less than 0.5 g/kWh (EURO VI level). Moreover, the amount of formaldehyde is also reduced to below 0.012 g/kWh (i.e., 2007 EPA level). Due to the high flammability properties of DME as well as the high burning rate of hydrogen, by using carbon dioxide produced in the reforming process of natural gas and also nitrogen addition as intake air-hydrogen mixture diluents (Figure 1), it is possible to control the excessive increase in in-cylinder temperature.

The average temperature inside the DME/Hydrogen fueled engine's combustion chamber can be controlled to less than 1600 K. As a result, the level of CO emission will increase to the relevant Euro II range (i.e., 4.0 g/kWh) due to the lower rate of oxidation of carbon monoxide to carbon dioxide resulting from the lower combustion rate (Table 10). In contrast, in the absence of diesel fuel consumption, soot formation is reduced to 0.1 g/kWh (Euro III level) under the influence of reduced combustion temperature and the use of the EGR. Moreover, it is expected that by reducing the temperature inside the combustion chamber to between 1500 K and 1600 K, the NOx emission level will decrease significantly. However, the excessive increase in local temperature in the DME ignition initiation zone, as an oxygenated fuel (about 35% by mass, Table 1); will cause a significant increase in this emission level to the Euro II range (i.e., 7 g/kWh).

5. Conclusions

In the present simulation study, in an RCCI engine at its mid-load range, the complete elimination of fossil fuel consumption (i.e., diesel fuel and natural gas) by replacing them with synthetic fuels (i.e., hydrogen and DME) produced from natural gas steam reforming process along with the use of intake mixture dilution can lead to the following results:

1- A 100% reduction in the share of fossil fuel energy and the use of synthetic fuels instead leads to a three times increase in the total fuel cost per hour of DME/Hydrogen RCCI engine operation.

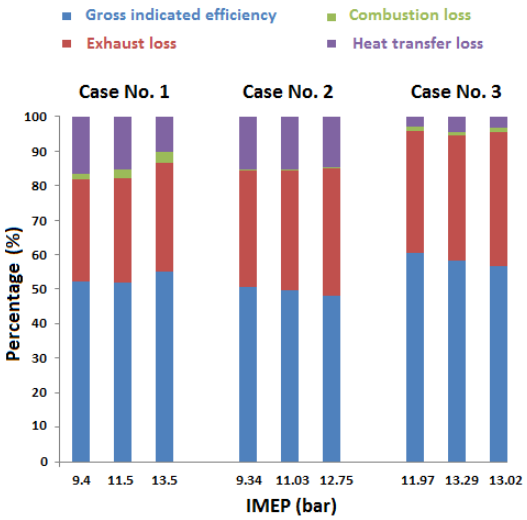

Figure 13. Comparative diagram of the energy balance for the three mentioned cases

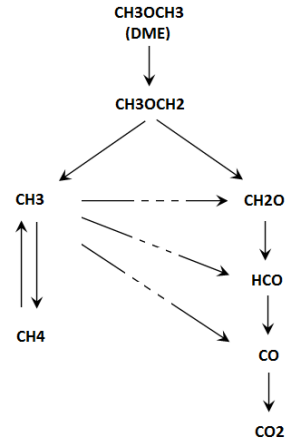

Figure 14. DME oxidation pathway

2- The necessity of DME injection at the TDC causes shifting the location of CA50 to more than 15 degrees of crank angle after the TDC and increases the combustion duration by about two times compared to fossil fuel engines.

3- Without any diesel knock, the maximum pressure in a fossil fuel-free engine's cylinder can be reduced by up to 30%. In contrast, the engine indicated means effective pressure can be increased by up to 27%.

4- In a DME/hydrogen RCCI engine, the gross indicated efficiency to more than 55% is achievable.

5- In a DME/hydrogen engine, energy losses due to the exhaust of the combustion products increase. Also, due to the decrease in the combustion rate resulting from the expansion effect, losses due to combustion inefficiency will increase.

6- In a single-cylinder DME/hydrogen-fueled engine, carbon dioxide as greenhouse gas emission can be reduced by up to 157 tons in a year in a continuous engine operation.

7- Although the combustion nature of DME as an oxygen-containing fuel increases NOx emission, the inefficiency of the overall combustion process increases CO emission.

Authors Contribution
All authors have contributed equally to prepare the paper.

Availability of data and materials
The data that support the findings of this study are available from the corresponding author, upon reasonable request.

Conflict of interests
The authors have no relevant financial or non-financial interests to disclose

References

1. The International Council on Combustion Engines, CIMAC, Guide to Diesel Exhaust Emissions Control of NOx, SOx, Particulates, Smoke and CO2, 2008.
2. Weaver C, Turner S. Dual Fuel Natural Gas/Diesel Engines: Technology, Performance, and Emissions. SAE Technical Paper 1994; 940548, DOI: https://doi.org/10.4271/940548
3. CIMAC, the International Council on Combustion Engines. Methane and Formaldehyde Emissions of Gas Engines, CIMAC position paper WG 17, 2014-04.
4. Duan H, Jia M, Li Y, Wang T. A comparative study on the performance of partially premixed combustion (PPC), reactivity-controlled compression ignition (RCCI), and RCCI with reverse reactivity stratification (R-RCCI) fueled with gasoline and polyoxymethylene dimethyl ethers (PODEn). Fuel 2021; 298: 120838.
5. Kokjohn SL, Musculus MPB, Reitz R D. Evaluating Temperature and Fuel Stratification for Heat Release Rate Control in a Reactivity-Controlled Compression-Ignition Engine using Optical Diagnostics and Chemical Kinetics Modeling. Combustion and Flame 2015; 162 (6): 2729-2742.
6. Li Y, Jia M, Xu L, Song Bai X. Multiple-objective optimization of methanol/diesel dual-fuel engine at low loads: A comparison of reactivity controlled compression ignition (RCCI) and direct dual fuel stratification (DDFS) strategies. Fuel 2020; 262: 116673.
7. Dalha I, Said M, Abdul karim A, El-Adawy M. Effects of port mixing and high carbon dioxide contents on power generation and emission characteristics of biogas-diesel RCCI combustion. Applied Thermal Engineering 2021; 198: 117449.
8. Baškovič UZ, Vihar R, Opršnik SR, Seljak T, Katrašnik T. RCCI combustion with renewable fuel mix-Tailoring operating parameters to minimize exhaust emissions. Fuel 2022; 311: 122590.
9. Walker NR, Wissink ML, Delvescovo DA, Reitz RD. Natural Gas for High- Load Dual-fuel RCCI in Heavy- Duty Engines. Journal of Energy Resources Technology 2015; 137: 042202-1-7.
10. Elkelawy M, Shenawy EAE, Mohamed SA, Elarabi MM, Bastawissi HAE. Impacts of using EGR and different DI-fuels on RCCI engine emissions, performance, and combustion characteristics. Energy Conversion and Management 2022; 15: 100236.
11. Ebrahimi M, Najafi M, Jazayeri SA. Multi-input multi-output optimization of reactivity-controlled compression-ignition combustion in a heavy-duty diesel engine running on natural gas/diesel fuel. International Journal of Engine Research 2020; 21(3): 470-483.
12. Kumar V, Gupta D, Kumar N. Hydrogen use in internal combustion engine: A review. International Journal of Advanced Culture Technology 2015; 3(2): 87-99.
13. Pielecha I, Engelmann D, Czerwinski J. Use of hydrogen fuel in drive systems of rail vehicles. Rail Vehicles/Pojazdy Szynowe 2022; 1(2): 10-19. DOI: https://doi.org/10.53502/RAIL-147725
14. Mabadi Rahimi H, Jazayeri SA, Ebrahimi M. Hydrogen Energy Share Enhancement in a Heavy Duty Diesel Engine under RCCI Combustion Fueled with Natural Gas and Diesel Oil. International Journal of Hydrogen Energy 2020; 45(35): 17975-17991.
15. Watgave S, Banapurmath N, Harari, P. Comparative Study on Effect of Hydrogen and Hydrogen Blended Compressed Natural Gas on Compression Ignition Engine Operated under Homogeneous Charge Compression Ignition and Reactivity Controlled Compression Ignition Mode of Combustion. SAE Technical Paper 2021; 28:0010.
16. Ebrahimi M, Jazayeri SA. Effect of hydrogen addition on RCCI combustion of a heavy duty diesel engine fueled with landfill gas and diesel oil. International Journal of Hydrogen Energy 2019; 44(14): 7601-7615.
17. Sattarzadeh M, Ebrahimi M, Jazayeri SA. A detail study of a RCCI engine performance fueled with diesel fuel and natural gas blended with syngas with different compositions. International Journal of Hydrogen Energy 2022; 47(36): 16283.
18. Jafari B, Seddiq M, Mirsalim SM. Impacts of diesel injection timing and syngas fuel composition in a heavy-duty RCCI engine. Energy Conversion and Management 2021; 247: 114759.
19. Liu L, Lin Z, Lin S, Chen Y, Zhang L, Chen S, Zhang X, Lin J, Zhang Z, Wan S, Yong Wang. Conversion of syngas to methanol and DME on highly selective Pd/ZnAl2O4 catalyst. Journal of Energy Chemistry 2021; 58: 564.
20. Zhen X, Wang Y. An overview of methanol as an internal combustion engine fuel. Renewable and Sustainable Energy Reviews 2015; 52: 477-493.
21. Yoon H, Kitae Yeom K, Bae C. The Effects of Pilot Injection on Combustion in Dimethyl-ether (DME) Direct Injection Compression Ignition Engine. SAE Thechnical Paper 2007; 24:0118.

22. Wang L, Liu J, Ji Q, Sun P, Li J, Wei M, Liu S. Experimental study on the high load extension of Polyoxymethylene dimethyl ethers/Methanol RCCI combustion mode with optimized injection strategy. Fuel 2022; 314: 122726.

23. Duraisamy G, Rangasamy M, Govindan N. A comparative study on methanol/diesel and methanol/ Polyoxymethylene dimethyl ethers (PODE) dual fuel RCCI combustion in an automotive diesel engine. Renewable Energy 2020; 145: 542-556.

24. Rangasamy M, Duraisamy G, Govindan N, Vaidhyanathan Y, Sellamuthu B. Experimental Investigation on Reactivity-Controlled Compression Ignition Combustion Using Simple and Similar Molecular Fuels—Methanol and Dimethyl Ether. SAE Int. J. Engines 2022; 15(1): 147-164.

25. Gharehghani A, Kakoee A, Andwari AM, Megaritis T, Pesyridis A. Numerical Investigation of an RCCI Engine Fueled with Natural Gas/Dimethyl-Ether in Various Injection Strategies. Energies 2021; 14(6):1638.

26. Faingold G, Tartakovsky L, Frankel SH. Numerical Study of a Direct Injection Internal Combustion Engine Burning a Blend of Hydrogen and Dimethyl Ether. Drones 2018; 2(3):23.

27. Li Y, Su S, Wang L, Yin J, Idiaba S. Reduction and optimization for combustion mechanism of dimethyl ether–air mixtures. International Journal of Chemical Kinetics 2022; 54(3): 142-153.

28. Luo Y, He Y, Liu C, Liao S.Combustion characteristics of biodiesel with different dimethyl ether blending strategies. Fuel 2023; 332 (Part 1): 126078.

29. Leblanc S, M M, Han X, Tjong J. Performance and Emission Characteristics of Direct Injection DME Combustion under Low NOx Emissions. SAE Technical Paper 2023; 01: 0327.

30. Agarwal AK, Mehra S, Valera H, Mukherjee NK, Kumar V, Nene D. Dimethyl ether fuel injection system development for a compression ignition engine for increasing the thermal efficiency and reducing emissions. Energy Conversion and Management 2023; 287: 117067.

31. Zubel M, Lehrheuer B, Pischinger S. Impact of increased injector nozzle hole diameters on engine performance, exhaust particle distribution and methane and formaldehyde emissions during dimethyl ether operation. International Journal of Engine Research 2021; 22(2): 503-515.

32. Sattarzadeh M, Ebrahimi M, Jazayeri SA. Maximum Reduction in Greenhouse Gas Emissions by Complete Replacement of Natural Gas with Pure Hydrogen as a Sole Low Reactive Fuel in a RCCI Engine. International Journal of Engine Research 2023; 24(6): 2677-2691.

33. Jia M, Bai J, Duan H, Li Y, Cai Y, Chang Y. Potential of hydrogen/diesel reactivity controlled compression ignition (RCCI) combustion from the perspective of the second law of thermodynamics. International Journal of Engine Research 2022; 23(5): 907-923.

34. Duan H, Jia M, Xu Z, Li Y, Xia G. Comprehensive analysis of combustion behaviors of hydrogen (H_2)/diesel reactivity-controlled compression ignition (RCCI) in a light-duty diesel engine. Fuel 2023; 353: 129237.

35. Karimi M, Wang X, Hamilton J, Negnevitsky M. Numerical investigation on hydrogen-diesel dual-fuel engine improvements by oxygen enrichment. International Journal of Hydrogen Energy 2022; 47(60): 25418-25432.

36. Rahimi A, Fatehifar E, KhoshbakhtiSaray R. Development of an Optimized Chemical Kinetic Mechanism for Homogeneous Charge Compression Ignition Combustion of a Fuel Blend of N-heptane and Natural Gas Using a Genetic Algorithm. Proc Institution Mech. Eng. Part D J Automobile Eng 2010; 224 (9): 1141-1159.

37. Gosman AD, Ioannides E. Aspects of Computer Simulation of Liquid- Fueled Combustor. AIAA1983; 7(6): 482-490.

38. Naber JD, Reitz RD. Modeling Engine Spray/ Wall Impingement. SAE 1988; 880107: 1-26.

39. Dukowicz JK. Quasi- Steady Droplet Change in the Presence of Convection. Informal report Los Alamos Scientific Laboratory, LA7997-MS1979.

40. Liu AB, Reitz RD. Modeling the Effects of Drop Drag and Break-up on Fuel Sprays. SAE 1999; 930072: 1-13.

41. Kunsberg- Sarre CV, Kong SC, Reitz RD. Modeling the Effects of Injector Nozzle Geometry on Diesel Sprays. SAE paper1999; 01-0912.

42. Eng JA. Characterization of pressure waves in HCCI combustion. SAE Technical Paper 2002; No. 2002-01-2859.

43. Ando H, Yasuyuki S. Universal Rule of Hydrocarbon Oxidation. SAE Paper 2009; 01-0948.

44. Chemical-kinetic mechanisms for combustion applications http://web.eng.ucsd.edu/mae/groups/combustion/mechanism. html

45. Li J, Zhao Z, Kazakov A, Dryer FL. An updated comprehensive kinetic model of hydrogen combustion. Int J Chem Kinet 2004; 36:1-10.

46. Wang H, You X, Joshi AV, Davis SG, Egolfopoulos F, Law CK. USC Mech version II. High-temperature combustion reaction model of H_2/CO/C1-C_4 compounds. http://ignis.usc.edu/USC_Mech_II.htm; May 2007

47. Kaiser EW, Wallington TJ, Hurley MD, Platz J, Curran HJ, Pitz WJ, Westbrook CK. Experimental and Modeling Study of Premixed Atmospheric-Pressure Dimethyl ether-Air Flames. Journal of Physical Chemistry 2000; A 104(35): 8194-8206. https://www.imarcgroup.com/hydrogen-pricing-report